Tuijin Jishu/Journal of Propulsion Technology
ISSN: 1001-4055
Vol. 44 No.4 (2023)

Application of Extreme Learning Machine (ELM) for Predicting Combustion Pressure-Related Parameters in a Dual Ignition Gasoline Engine

Suresh Shetty[1], Rashmi P Shetty[1*], Rahul Pai[2] Chennasappa Hampali[3], Basawaraj[4]

[1] *N.itte (Deemed to be University), NMAM Institute of Technology, Nitte-574110, Karnataka, India.*

[4]*School of Mechanical €engineering, REVA University, Bangalore, Karnataka, India*

[4] *Associate Professor, Dept of Aerospace Engineering, VIAT, VTU-Muddenahalli, Chikkaballapur, Karnataka, India.*

[2]*Chalmers University of Technology, Sweden.*

Abstract: The study focused on the development of Extreme Learning Machine (ELM) based Artificial Neural Network (ANN) model. The developed model then used for predicting combustion related cylinder pressure parameters of a spark ignition (SI) engine. A widely used back propagation (BP) based ANN model also developed for the prediction performance comparison. For training and testing the model, set of data has been collected by conducting the experiment on twin spark ignited SI engine. The experiment was carried out under different load, ethanol-gasoline blend, compression ratio and spark timing. The modelling results showed that ELM based ANN model gives minimum MSE and MAPE (%) compared to the BP based ANN model. It is also found that the ELM algorithm is faster as it takes only one epoch with added advantages of good generalization performance and compact network architecture.

***Keywords*:** ANN, ELM, BP, IMEP, COV

***Nomenclature and* Abbreviations**

[dP/dϴ]m	Maximum rate of pressure rise	ELM	Extreme learning machine
ANN	Artificial Neural Network	HC	Hydro Carbon
bTDC	Before TDC	HCCI	Homogeneous charged compression ignition
BP	Backpropagation	IGN	Ignition
BSFC	Brake-Specific Fuel Consumption	I_{mep}	Indicated Mean Effective Pressure
CAD	Crank Angle Degree	K-ELM	Kernel-ELM
c-b-c	Cycle–by–Cycle	MAPE	Mean Absolute Percentage Error
CFD	Computerised Fluid Dynamics	ANN	Artificial Neural Network
CO	Carbon Monoxide	MLP	Multilayer Perceptron
COV	Coefficient of variation	MSE	Mean Square Error

CR	Compression Ratio	NOx	Oxides of Nitrogen
DSI	Dual Spark Ignition	Pm	Maximum cylinder pressure
DI	Direct Injection	SI	Spark Ignition
E05	5% Ethyl alcohol +95% Petrol	TDC	Top Dead Centre
E10	10% Ethyl alcohol +90% Petrol	Ɵ	Crank angle
E15	15% Ethyl alcohol +85% Petrol	$\boldsymbol{\sigma}$	Standard deviation
E20	20% Ethyl alcohol +80% Petrol	S	Seconds
ECU	Electronic Control Unit	$\bar{X}$	Arithmetic mean

1 Introduction

Raising oil prices continuously and stringent emission regulations assist to use a higher percentage of ethanol in the gasoline. The higher blending ratio of ethanol not only saves money and lowered carbon emissions, but also increases energy security, good air quality, better use of damaged food grains, increases farmers' incomes and greater opportunities for capital investment, etc. [1]. The blending of ethanol with gasoline reduces the quantity of gasoline required for the engine and thereby reducing the dependency on costly imported petroleum derived fuels [2]. The higher blending of ethanol makes use of many supporting arguments, including the availability of large farming land, rising food grain and sugarcane production that is creating surpluses, the availability of technology to produce ethanol from plant-based sources, and the viability of making vehicles compliant with ethanol blended gasoline [3]. Due to the favorable characteristics of bioethanol, such as its higher-octane number, wider flammability limit, faster flame speed, and higher heat of vaporization, an engine can burn fuel more efficiently at a high compression ratio and shorter burn time [4-6]. Because the ethanol molecule contains oxygen in its molecular structure, it allows the engine to more completely combust the fuel, resulting in fewer emissions [4-8]. Previous studies have revealed that bioethanol in gasoline can improve engine performance while also lowering exhaust emissions without requiring major changes in the engine's design [9]. The presence of ethanol in the air fuel mixture forms the gasoline engine operation to a leaner air-fuel ratio since ethanol is an oxygenated fuel [10]. Even though lean mixture operation lowers fuel consumptions and tail pipe emissions, ultra-lean operation increases cycle-by-cycle (c-b-c) fluctuations which in turn causes rough engine operation and increased emissions [11-13]. Hence it is necessary to minimize c-b-c fluctuations of the engine when it is operated with ethanol as a fuel blend. There are many research works done either by experiment or simulation on the c-b-c fluctuations of the engine with regard to their occurrence, causes and remedies [14-17]. If these variations are eliminated, there would be a 10% increase of engine power output for the same fuel consumption as stated by the Soltau, J. P. [18]. Laminar flame burning velocity is one of the factors that mainly affect the engines c-b-c fluctuations [17]. The strategies that can accelerate laminar flame burning velocity will reduce the c-b-c fluctuations of the engines. There are several approaches for increasing the laminar flame burning velocity which includes combustion chamber shape optimization, optimization of spark plugs location and ignition at multiple points in the engine cylinder [19-20]. Out of all, a simple, comfortable and least expensive approach is the ignition at multiple points. This approach enhances the mixture burning speed and results in more combustion completeness [21].

A dual spark ignition [DSI] employs double spark plugs mounted in each engine cylinder at different locations and is commonly seen in aircraft engines [22], but is now also implemented in road vehicles. A DSI system initiates spark at different spots simultaneously in the burning zone and moves across the burning zone resulting in a shorter effective flame travel distance and hence boosting the knocking resistance of the engine. A DSI engine has shown an extended lean misfire limit in a carbureted single cylinder SI engine [23]. A DSI single cylinder SI engine, operating with CNG increased power output by 3-5% [24]. Raja et al. [25] experimentally showed that a DSI engine increases BSFC, volumetric efficiency, and excess air coefficient and reduces exhaust emissions such as CO, HC and NOx with increase in ethanol content in the fuel blend. Huichao Swang et al. [26]

investigated the impact of DSI on the combustion and knocking tendency of the engine. This work noticed that the DSI approach effectively improves the burning process and hence rises the peak pressure in the cylinder. Also, the DSI shortens the burning period and hence reduces the c-b-c variations. They finally concluded that the utility of DSI will be very beneficial under lean burn operation. Ismail Altın et al. [27] theoretically investigated the combustion behavior of a DSI engine with ethanol and concluded that a DSI engine's combustion behavior is similar to a centrally placed single plug operation. Aisyah et al. [28] investigated the usage of ethanol (94–100%) as fuel in DSI engines and compared it with a single plug operation. This work concluded that the presence of ethanol in dual spark plug operation yields more efficient combustion compared to single plug operation.

The intricate combustion process is affected by many unanticipated parameters. High precise instruments and equipment are needed for measuring these parameters, and it is necessary to conduct multiple tests for ascertaining the correlation between various parameters [29]. A lot of money and effort must be spent on these kinds of tests. The correlation between each engine parameter might be difficult to identify by employing simple mathematical equations with assumptions and simplifications [29,30]. These difficulties can be resolved by employing ANN approaches [31]. An ANN is a computing system in which the information is processed in a fashion same as human brain by using artificial neurons [32]. ANN detects the necessary information about the underlying problem by learning non-linear correlations that are hidden inside the problem domain [33-34].

A Multilayer Perceptron (MLP) Neural network is a feed-forward neural network which consists of nodes in every layer with every layer linked to the subsequent layer. The MLPNN is appropriate for finding complicated non-linear relationships. MLPNN uses BP learning approach to train the network [35]. Traditional ANN models employ a gradient descent learning process, that is usually slow and needs iterative network parameter tuning. Further, it has a proclivity to converge to local minima [36]. G.B Haung [37] developed the ELM algorithm, which is a fast batch learning algorithm with good generalization performance involving smaller number of simulation parameters. ELM learning uses a single-pass process, that makes it extremely fast as it removes the iterative method associated with the gradient descent learning algorithm [39]. Further, the non-iterative nature of this technique helps it in overcoming local minima problems. Hence it is a better choice for large-scale computing for real time applications [38]

A.H. Sebayang et al. [40] proved that the coefficient of determination (R^2) is within a range of 0.980–1.000 and the MAPE values within a range of 0.411%−2.782%, indicating that the ANN model developed by the ELM algorithm is capable of prediction of engine performance as well as exhaust emission parameters in bioethanol-gasoline fueled SI engine. Weiying Zeng et al. [41] presented an ANN approach to predict gasoline engine output torque with good accuracy using an ELM based single-hidden layer feedforward neural network. Viviana C. M. et al. [42] predicted the pressure of SI engines using optimized ELM models and presented that the proposed model and its variants optimized by biogeography-based optimization approaches have the potential to predict IMEP at reasonable consistency with experimental results. A.S. Silitonga et al. [43] used K-ELM to predict performance parameters as well as emission parameters of the engine. MAPE (%) of the parameters predicted by the K-ELM model was within 1.363– 4.597%, whereas the R^2 values were close to one. They concluded that K-ELM was a reliable technique to predict the performance and exhaust emission parameters of engines fueled with biodiesel-bioethanol-diesel blends. ELM model is also applicable in a variety of research areas, including the development of a model for combustion knocks probability control of SI engines [44], predictive control method for homogeneous charged compression ignition (HCCI) engines [45], predicting engine performance in a direct injection diesel engine running on diesel/biodiesel blends containing polymer waste [46] etc.

It is understood from the literature survey that there are only a few studies on DSI engines using ethanol-gasoline blends as fuel. It is also observed that the vast majority of them are related to engine performance studies and few are on combustion studies. In addition to this, the majority of the studies included the BP algorithm to predict engine performance, emission and combustion related parameters. The studies focused to predict combustion related parameters using ELM are found to be limited. Thus, the aim of present work is to develop an efficient ELM model for the prediction of combustion related parameters of DSI engines fueled with ethanol-gasoline blends and then compare the performance with the widely used BP algorithm model.

2 Materials and Methods

2.1 Fuel Preparation and Properties

In this study, different blends of gasoline (REC-90) and ethanol (99.9% pure) has been prepared to conduct experiment on SI engine in order to acquire data for training and to test the model. This gasoline and ethanol were mixed in different proportions such as 100-0%, 95-5%, 90-10%, 85-15% and 80-20% by volume and are represented as pure gasoline, E5, E10, E15 and E20 respectively. Using magnetic stirrer, the mixture is agitated under 500-600 rpm speed for about 4-5 minutes to obtain uniform mixture. The physical, chemical and thermal properties of blends obtained from the literature [51] are listed in Table 1.

Table 1 Properties of Ethanol-Gasoline Blends

Properties	Gasoline	Ethanol	E05	E10	E15	E20
Specific gravity	0.772	0.770	0.773	0.775	0.776	0.777
Carbon (% mass)	87.4	52.4	87.7	86.7	87.6	87.6
Hydrogen (%mass)	15.8	13	12.2	13.2	12.3	12.3
Oxygen (%mass)	0.00	34.73	1.89	3.97	5.86	7.89
Read vapour pressure at 37.8^0C (kPa)	173	60	59.3	59.6	58.8	58.3
Research octane number	90	108	92.8	93.6	95.3	105.6
Motor octane number	80	92	82.4	82.7	83.4	87.90
Stoichiometric AFR	14.57	8.94	14.26	13.96	13.36	13.00
Lower calorific value (KJ/kg)	42.61	26.90	40.57	39.82	39.41	39.00
Laminar burning velocity (cm/s)	34	42	34.42	34.88	35.32	35.74
Latent heat of vaporization (KJ/kg)	305	840	-	-	-	-
Auto ignition temperature (^{0}C)	442.8	257.2	265	271	281	290

2.2 Engine Setup and experimental procedure

The experimental set-up consists of a single-cylinder, four-stroke, liquid-cooled, variable compression ratio (VCR) DSI engine attached to an eddy current dynamometer. The schematic layout of the engine setup for gathering data is displayed in Fig.1. The technical specifications of the test engine are listed in Table 2.

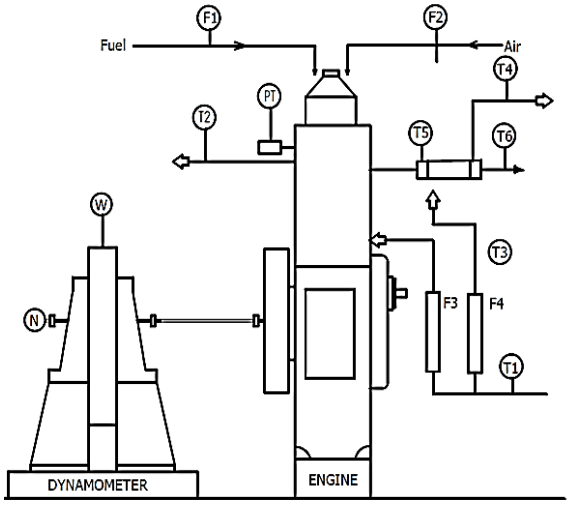

Fig.1 The layout of an experimental set-up

PT= Pressure transducer	T6 = EGT at the exit to the calorimeter
T1= Engine cooling water temperature at entry	F1= volume of fuel in m^3/s to the engine
T2 = Engine cooling water temperature at exit	F2 = volume of air in m^3/s to the engine
T3 = Water temperature at entry to the calorimeter	F3 = Volume of engine cooling water in $m^3/hr.$ at entry
T4 = Water temperature at exit to the calorimeter	F4 = Volume of water in $m^3/hr.$ at the calorimeter entry
T5 = EGT at the entry to the calorimeter	N = Crank angle encoder

The setup contains accessories for the measurement of combustion pressure in bar, crank angle in degrees, air and fuel flow rate in m^3/hr, temperature in K and engine load in kg. The data from these accessories are interfaced to a software through high speed data acquisition device. A programmable open ECU in the setup controls all the operating variables of the engine. The data collection and analysis were done using "engine soft" that is also compiled in the engine setup.

The engine was tested under different loads, blends, compression ratios and spark timings at 1800 rpm constant speed using open ECU mode. Under each operating condition, the data of IMEP, P_{max} and $[dP/d\theta]_{max}$ parameters have been acquired for 200 cycles once the engine cooling water reaches steady state temperature. Finally, the mean value ($\overline{X}$) and coefficient of variation (COV) of each parameter has been calculated using the Eq. (1) and (2) respectively [49-52].

$$\overline{X} = \frac{\sum_{i=1}^{N} X_i}{N} \quad (1)$$

$$\sigma = \sqrt{\left(\sum_{i=1}^{N} \left(X_i - \overline{X}\right)^2 / N\right)}$$

$$COV = \frac{\sigma}{\overline{X}} \quad (2)$$

Where

N = Sample size

σ = Standard deviation

Table 2 Engine specification.

Engine type	4-stroke, Multifuel, VCR engine with DSI and open ECU (computerized)
Rated Power	4.5kW
Rated Speed	1500 rpm
Cooling system	Water-cooled
Bore	87.5mm
Stroke	110 mm
Compression Ratio	Variable 6:1 to10:1
Swept volume	661 cc
Dynamometer	Water-cooled eddy current with loading unit
Dynamometer arm length	185 mm

2.3 Engine testing conditions

To acquire data for training and test the model, different engine testing conditions have been employed. The engine test protocol included measurements at different ethanol-gasoline blends, engine loads, compression ratios and spark timings, which are listed in the Table 3. All the variables are measured at a constant speed of 1800 rpm.

Table 3 Engine testing environment

Fuel blends [% volume]	0 [Pure gasoline], 5 [E5], 10 [E10], 15 [E15] and 20 [E20]
Spark timing [^{0}bTDC]	20^0-20^0, 24^0-24^0 and 28^0-28^0
Compression ratio	8:1, 9:1 and 10:1
Load (% full load)	60, 80 and 100
Speed	Constant 1800 rpm

3 ELM Model

MLP is a popular and universally accepted type of neural network. It is a simplest form of neural network working only in forward direction. It can handle complex non-linear problems while dealing with large data sets. The sigmoidal activation function in MLP introduces this nonlinearity, allowing the network to learn complex relationships. Some other characteristic feature of MLP is the high degree of connectivity decided by the synapses of the network [52].

Back Propagation (BP) learning algorithm is a well-known and broadly used error-correction learning algorithms. But there are numerous shortcomings in the BP algorithm. The primary one is its iterative nature which makes the convergence extremely slow. The algorithm tends to regularly converge to local minima. This factor turns highly undesirable if the difference between global and local minima is massive. Defining the stopping criterion will become crucial in error minimization learning algorithm. Otherwise, the network may get over-trained and can bring about bad generalization performance [37,53]. Further, fixing the proper values for learning rate (η) and momentum rate (α) parameters play an important role in the convergence and the performance of this algorithm [54].

ELM is a simple yet effective and non-iterative algorithm, which is finding significance in real-time applications involving complexity and massive computations because of its excellent generalization ability, remarkable efficiency, universal approximation and simplicity [37]. To achieve the output weight matrix, the algorithm makes use of a generalized inverse (Moore- Penrose) operation on the output matrix of the hidden layer. This algorithm is powerful and easy because it involves a smaller number of simulation parameter in comparison to traditional gradient descent learning algorithms. Less number of simulation parameters leads to less human intervention for tuning those parameters. Furthermore, this algorithm has established its ability in a huge variety of applications with good generalization performance [55,56]. Further, ELM requires the only one epoch for training, and thus proves to be extraordinarily faster in comparison with the gradient descent technique [57]. Some of the application of this algorithm is in fields such as system identification, control and robotics, computer vision, biomedical engineering etc. [58].

The working of the ELM algorithm is as follows:

Choose a set of input and output $\{x_i^{\mu}, y_k^{\mu}\}$ from the training patterns.

Where, $\mu = 1, 2...N$ constitutes a number of patterns.

$i = 1, 2...p$ constitutes a number of input attributes and

$k = 1, 2...r$ constitutes a number of output attributes.

1. The weights and bias i.e., w_{ji}, b_{jk} values are initialized randomly.

2. Determine hidden layer output using equation (3) for Q number of hidden nodes.

$$H(w_1, \dots w_N, b_1, \dots . b_N, x_1, \dots \dots x_N) = \begin{bmatrix} g(w_1 x_1 + b_1) & \dots & g(w_Q x_1 + b_Q) \\ . & & . \\ . & \dots & . \\ . & & . \\ g(w_1 x_N + b_1) & \dots & g(w_Q x_N + b_Q) \end{bmatrix}_{NXQ} \quad (3)$$

Where $g(x)$is the activation function, which is usually a sigmoidal activation function.

3. Obtain the output weight matrix w_{kj}: $w_{kj} = H^{\dagger}T$,

where $H^{\dagger}$ is the Moore-Penrose generalized inverse of the H, and T is the actual output matrix as given in equation (4) [53].

$$T = \begin{bmatrix} t_1^T \\ . \\ . \\ . \\ t_N^T \end{bmatrix}_{NXk} \quad (4)$$

The collected experimental data have been used for training and to test the model. From the collected data, 85% has been used for training and the remaining 15% for testing the model developed. The data were normalized between zero and one using equation (5) so that all inputs exert an equivalent influence on the development of the ANN model.

$$X' = \frac{X}{X_{Max}} \quad (5)$$

Where X', X and X_{Max} be the normalized data, original data and maximum data in the dataset respectively

Six different ANN models were developed in the present work. Model-1, Model-3 and Model-5 were developed using the BP learning algorithm and Model-2, Model-4 and Model-6 were developed using the ELM algorithm to predict IMEP, P_{max} and $[dP/d\theta]_{max}$ parameters respectively. Table 4 shows the details of these models.

Table 4 Details of ANN models

Model No.	Learning algorithm	Output parameter	Optimum configuration	η	α
Model-1	BP	I_{mep} and COV_{Imep}	4:35:2	0.023	0.015
Model-2	ELM	I_{MEP} and COV_{Imep}	4:25:2	-	-
Model-3	BP	$P_{ma,}$ COV_{pm} and Θ_{pm}	4:35:3	0.030	0.016
Model-4	ELM	$P_{ma,}$ COV_{pm} and Θ_{pm}	4:20:3	-	-
Model-5	BP	$[dP/d\Theta]_{m,}$ $COV_{[dP/d\Theta]m,}$ and $\Theta_{[dP/d\Theta]m}$	4:40:3	0.028	0.018
Model-6	ELM	$[dP/d\Theta]_{m,}$ $COV_{[dP/d\Theta]m,}$ and $\Theta_{[dP/d\Theta]m}$	4:25:3	-	-

The % load, % blend, compression ratio and spark timing are used as the model input parameters to predict parameters of IMEP, maximum cylinder pressure, and maximum rate of pressure rise.

(a) (b) (c)

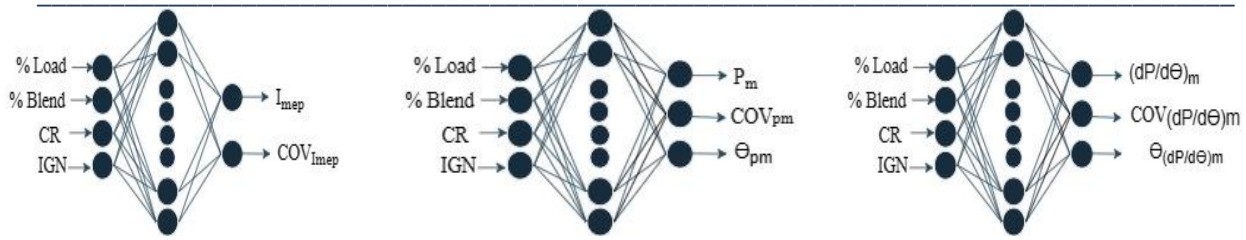

Fig. 2 General architectures of ANN model to predict (a) I_{MEP} (b) P_m (c) $[dP/d\Theta]_m$ parameters.

Fig. 2(a), Fig. 2(b) and Fig. 2(c) represent the general architecture of the ANN model to predict IMEP parameters, P_{max} parameters and $[dP/d\theta]_{max}$ parameters respectively. The simulations were carried out on a personal computer by customized codes in MATLAB R2014a environment with an Intel i5-6200U, 2.3 GHz CPU and 4 GB RAM.

The methodology adopted in this study is shown in Fig. 3. Three models Model-1, Model-3 and Model-5 were trained using the BP algorithm. In this work, the minimum error or maximum number of epochs were the criteria used for stopping network training. The value for these criteria has been fixed as $1 * 10^{-3}$and 1000 respectively. The value of simulation parameters, η and α for MLP were fixed based on a trial and error during training, according to maximum prediction accuracy. Training the models has been done for different hidden layer size. The best values have been provided in Table 4.

Three models Model-2, Model-4 and Model-6 were trained by using the ELM algorithm. The most interesting feature of ELM is that it takes only a single epoch for network training and it involves few numbers of model simulation parameters. The only simulation parameter for training the ELM model is the number of neurons of hidden layers that have been fixed on a trial and error technique by taking into account the maximum training accuracy. The optimum configurations along with simulation parameters of all the models are given in Table 4.

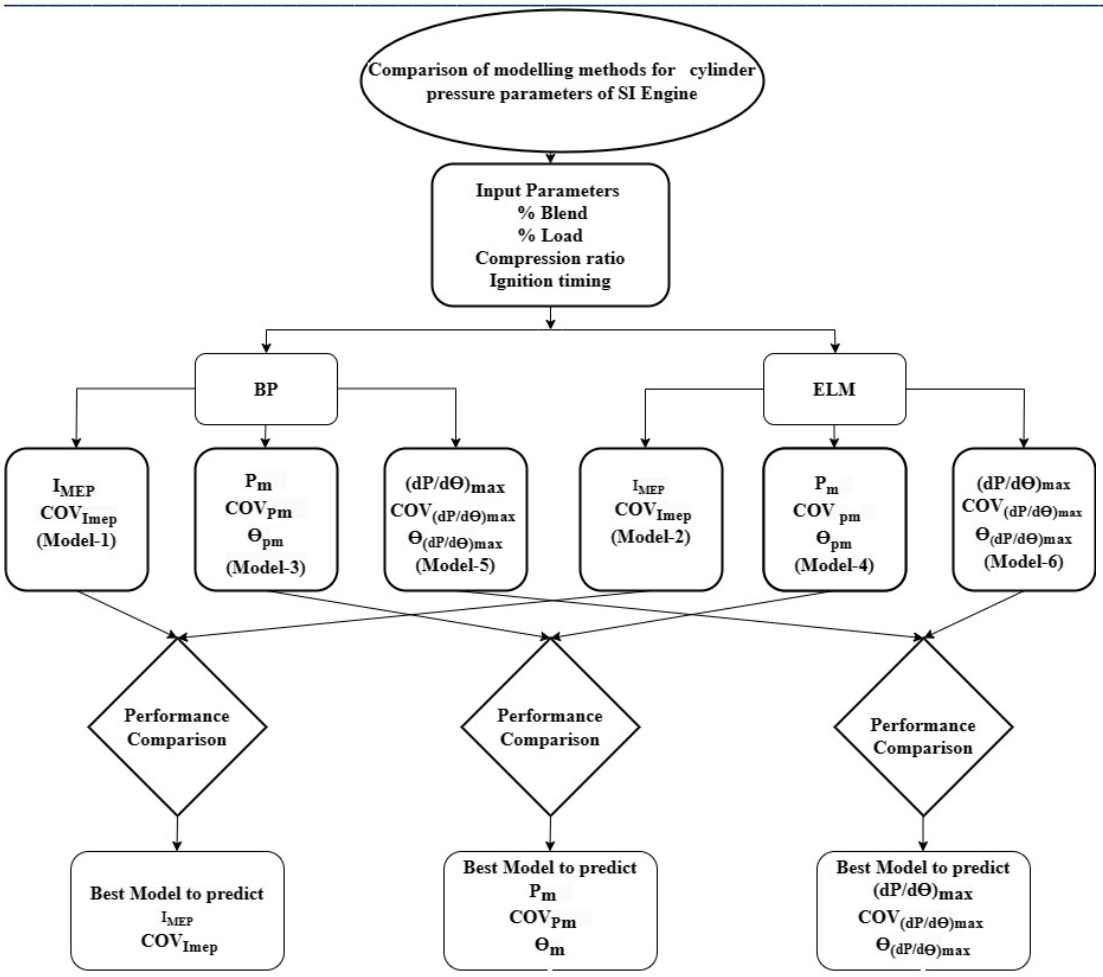

Fig. 3 Methodology adapted in this work

4 Results and Discussions

In this study, six ANN models have been developed and the results are compared to obtain the best ANN model. Three models, Model-1, Model-3 and Model-5 were developed using the BP learning algorithm and Model-2, Model-4 and Model-6 were developed using the ELM learning algorithm for three different sets of output parameters namely i) I_{mep} and $COV_{Imep,}$ ii) $P_{m,}$ COV_{pm} and θ_{Pm} iii) $[dP/d\Theta]_{m,}$, $COV_{[dP/d\Theta]m}$ and $\theta_{[dP/d\Theta]m}$. The performance of the models was assessed using two performance metrics namely MAPE (%) and MSE which are determined using Equation (6) and Equation (7) respectively.

$$\text{MAPE}\ (\%) = \frac{1}{N}\sum_{i=1}^{N}\frac{|y_p(i)-y_a(i)|}{y_a(i)} \times 100 \quad (6)$$

$$MSE = \frac{1}{N}\sum_{i=1}^{N}\ (y_p(i) - y_a(i))^2 \quad (7)$$

Where $y_p(i)\ and\ y_a(i)$ represent predicted values and actual values respectively of the output parameter at the i^{th} data point and N constitutes the total number of data points considered.

4.1 I_{mep} and COV_{Imep} Prediction Model

Model-1 and Model-2 were developed for the prediction of the IMEP parameters i.e. I_{mep} and COV_{Imep}. The result of these two models are shown in Table 5 and Table 6 respectively.

Table 5 Performance of Model-1 for the prediction of I_{mep} and COV_{Imep}

Hidden layer size	25	30	**35**	40	45	50
Training set MSE	0.00097	0.00084	**0.00075**	0.00092	0.00099	0.0015
Test data MSE	0.0019	0.0015	**0.00088**	0.0017	0.0025	0.0030
Training set MAPE (%)	8.11	6.75	**5.66**	7.98	9.75	10.55
Test data MAPE (%)	11.91	10.94	**8.38**	11.39	11.98	12.01
Execution Time (s)	0.505001	0.525827	**0.596251**	0.60517	0.645477	0.671810

Table 6 Performance of Model-2 for the prediction of I_{mep} and COV_{Imep}

Hidden layer size	15	20	**25**	30	35	40
Training set MSE	0.00065	0.00050	**0.00020**	0.00031	0.00045	0.00055
Test data MSE	0.00078	0.00072	**0.00033**	0.00042	0.00056	0.00061
Training set MAPE (%)	4.92	3.54	**1.77**	2.80	3.12	4.95
Test data MAPE (%)	7.98	6.31	**2.33**	3.95	4.80	6.46
Execution Time (s)	0.003945	0.004061	**0.004095**	0.004207	0.004431	0.004662

For Model-1 as well as Model-2, the hidden size was set manually, and the results are displayed for the varied hidden layer size. It can be noticed that Model-1 resulted in the least MAPE (%) value of 8.38 on test set for hidden layer size of 35 neurons using 0.596251 seconds of Execution time. Whereas Model-2 presented the best result for hidden layer size of 25 neurons with the least MAPE (%) of 2.33 on test set taking 0.004095 seconds of Execution time. It can be realized that Model-2 is an accurate and compact model with extremely fast learning compared to Model-1.

(a) (b)

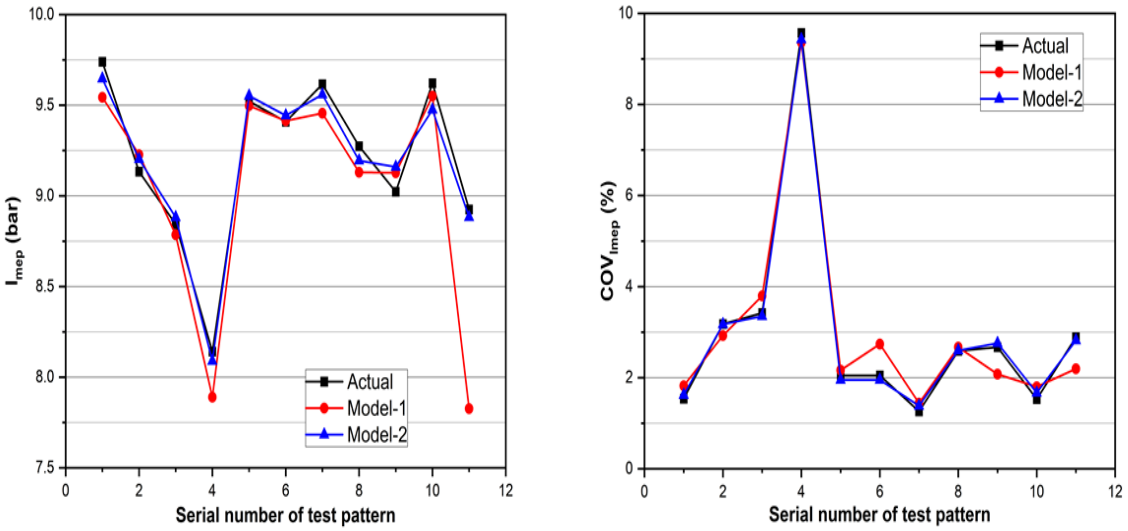

Fig. 4 Comparison of Actual Vs Predicted (a) I_{MEP} and (b) COV_{Imep} for Model-1 and Model-2

The comparison of IMEP and COV_{IMEP} predictions achieved from these two models with the actual is represented in Fig. 4(a) and Fig. 4(b) correspondingly. In both cases, it can be viewed from the figure that the actual and the predicted values of Model-2 are in good agreement compared to Model-1. This demonstrates the superiority of the ELM model in providing better performance than the BP model.

4.2 P_{ma}, COV_{pm} and Θ_{pm} Prediction Models

Model-3 and Model-4 were developed for the prediction of maximum cylinder pressure parameters i.e. P_{ma}, COV_{pm} and Θ_{pm}. Table 7 and Table 8 presents the results of Model-3 and Model- 4 respectively.

Table 7 Performance of Model-3 for the prediction of P_{ma}, COV_{pm} and Θ_{pm}

Hidden layer size	15	20	25	30	**35**	40
Training set MSE	0.00098	0.00087	0.00084	0.00079	**0.00047**	0.00055
Test set MSE	0.0025	0.0019	0.00093	0.00086	**0.00059**	0.00074
Training set MAPE (%)	12.21	10.11	9.48	8.01	**6.52**	7.38
Test set MAPE (%)	18.25	16.23	14.4	12.01	**9.39**	11.17
Execution Time (s)	0.520462	0.431690	0.245194	0.317968	**0.291639**	0.264371

Table 8 Performance of Model-4 for the prediction of P_{ma}, COV_{pm} and Θ_{pm}

Hidden layer size	5	10	15	**20**	25	30
Training set MSE	0.00028	0.00021	0.00016	**0.00013**	0.00011	0.00025
Test set MSE	0.00040	0.00037	0.00032	**0.00022**	0.00029	0.00034
Training set MAPE (%)	5.21	5.11	4.48	**1.93**	3.66	4.38
Test set MAPE (%)	9.42	8.79	6.88	**3.24**	4.94	6.18
Execution Time (s)	0.004746	0.004711	0.006950	**0.008585**	0.006908	0.004529

(a)

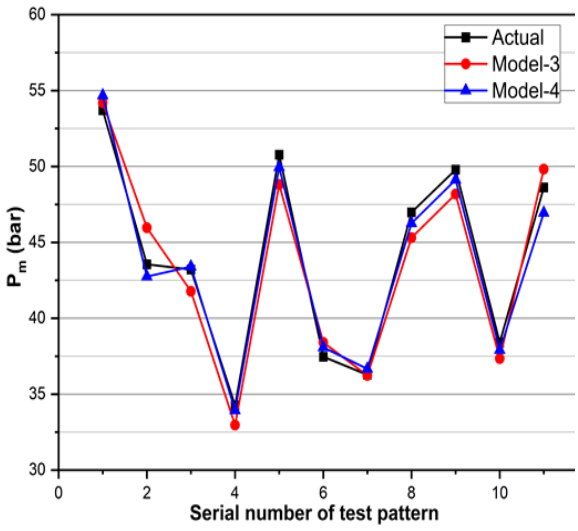

(b)

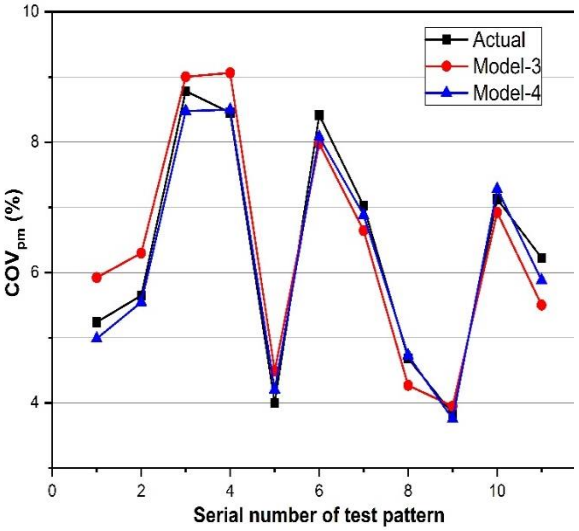

(c)

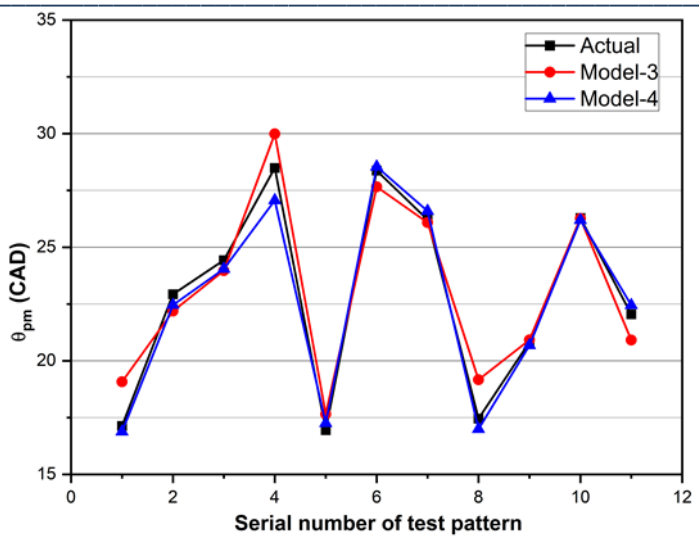

Fig. 5 Comparison of Actual Vs Predicted (a) P_{ma}, (b)COV_{pm} and (c) Θ_{pm} for Model-3 and Model-4

In case of both the models, the error is found to be decreasing with the increase in hidden layer size up to a certain value i.e 35 and 20 respectively for Model-3 and Model-4 and increased thereafter. Model-4 recorded a minimum MAPE error (%) of 3.24 on test set with 20 hidden neurons taking 0.008585 seconds since it uses the ELM algorithm. Fig. 5(a), Fig. 5(b) and Fig. 5(c) illustrate the comparison of predicted values of two models with the actual for Pmax, COV_{Pmax} and θ_{Pmax} respectively. From the graph, it can be realized that Model- 4 performs better compared to Model-3 with predicted values close to the actual values.

4.3 $[dP/d\Theta]_m$, $COV_{[dP/d\Theta]m}$, and $\Theta_{[dP/d\Theta]m}$ Prediction Models

Two Models Model-5 and Model-6 were developed for the prediction of $[dP/d\Theta]_m$, $COV_{[dP/d\Theta]m}$, and $\Theta_{[dP/d\Theta]m}$.

The performance of these two models is represented in Tables 9 and Table 10 respectively for a varied hidden layer size.

Table 9 Performance of Model-5 for the prediction of $[dP/d\Theta]_m$, $COV_{[dP/d\Theta]m}$, and $\Theta_{[dP/d\Theta]m}$

Hidden layer size	25	30	**40**	45	50	55
Training set MSE	0.00092	0.00082	**0.00077**	0.00087	0.0013	0.0018
Test set MSE	0.0017	0.0011	**0.00092**	0.0017	0.0022	0.0025
Training set MAPE (%)	8.12	6.74	**5.82**	7.97	9.76	10.56
Test set MAPE (%)	11.90	10.93	**8.87**	11.38	11.99	12.02
Execution Time (s)	0.421601	0.568571	**0.596922**	0.680706	0.840428	0.876413

Table 10 Performance of Model-6 for the prediction of $[dP/d\Theta]_m$, $COV_{[dP/d\Theta]m}$, and $\Theta_{[dP/d\Theta]m}$

Hidden layer size	5	10	15	20	**25**	30
Training set MSE	0.00065	0.00042	0.00039	0.00034	**0.00022**	0.00025
Test set MSE	0.00082	0.00075	0.00061	0.00048	**0.00036**	0.00041
Training set MAPE (%)	5.03	4.27	3.32	2.99	**1.17**	3.05
Test set MAPE (%)	8.73	7.23	6.50	4.05	**2.80**	5.46

Execution Time (s)	0.004385	0.004601	0.004925	0.004703	**0.005494**	0.005826

Table 9 shows that the error for Model-5 decrease with an increase in hidden layer size and the minimum MAPE (%) value of 5.83 was achieved for 40 neurons taking 0.596921 seconds of Execution time. Consequently, for Model- 6, it was noticed that the least MAPE (%) for training was achieved with 25 hidden layers neurons, which took only 0.005494 seconds of Execution time since this is an ELM based model with only a single epoch. Fig. 6(a) through Fig. 6(c) shows the comparison of the performance of Model-5 and Model-6 respectively for test patterns of $[dP/d\theta]_{max,}$ COV $_{[dP/d\theta]max}$ and $\theta_{[dP/d\theta]max}$. From the figure, it can be realised that Model-6, the predicted values demonstrate a higher degree of proximity to the actual values in comparison to Model-5, which is a BP based model.

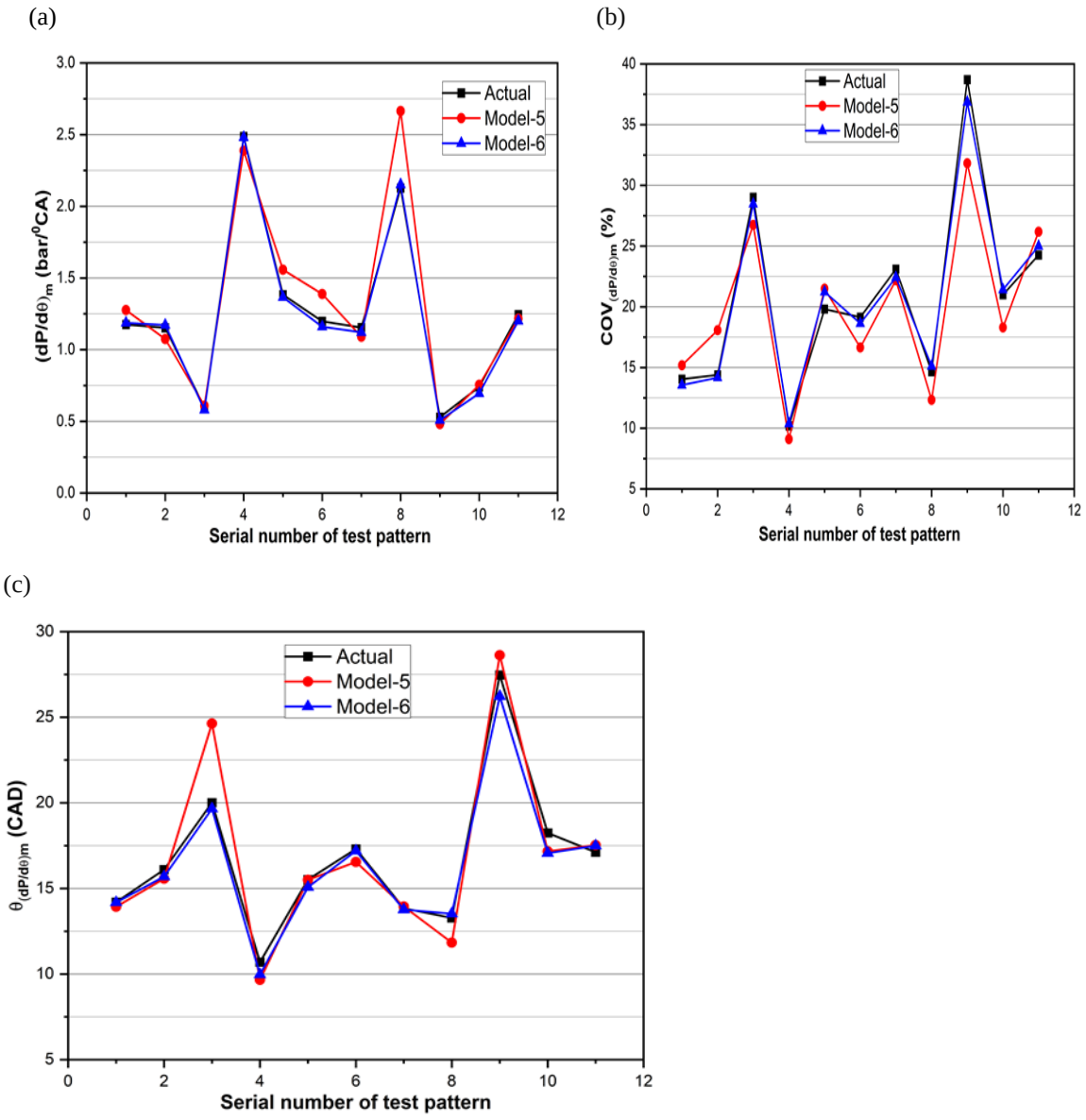

Fig. 6 Comparison of Actual Vs Predicted (a) $[dP/d\Theta]_{m,}$ (b) COV $_{[dP/d\Theta]m,}$ and (c) $\Theta_{[dP/d\Theta]m}$ for Model-5 and Model-6

4.4 Comparison of BP and ELM based models

The comparison of performance of BP and ELM models for Indicated Mean Effective Pressure (I_{mep}), Maximum cylinder pressure (P_m) and Maximum rate of pressure rise ($[dP/d\Theta]_m$) parameters has been presented in Table

11. Model-1, Model-3 and Model-5 are models using BP learning whereas Model-2, Model-4 and Model-6 are ELM based models.

Table 11 Comparison of performance of ANN models

Models	Output parameters	Learning algorithm	Hidden layer size	Training set MSE	Test set MSE	Training set MAPE (%)	Test set MAPE (%)	Execution Time (s)
Model-1	I_{MEP} and COV_{Imep}	BP	35	0.00075	0.00088	5.66	8.38	0.596251
Model-2		ELM	25	0.00020	0.00033	1.77	2.33	0.004095
Model-3	$P_{ma,}$ COV_{pm} and Θ_{pm}	BP	35	0.00047	0.00059	6.52	9.39	0.291639
Model-4		ELM	20	0.00013	0.00022	1.93	3.24	0.008585
Model-5	$[dP/d\Theta]_{m,}$ $COV_{[dP/d\Theta]m,}$ and $\Theta_{[dP/d\Theta]m}$	BP	40	0.00079	0.00091	5.83	8.88	0.596921
Model-6		ELM	25	0.00022	0.00036	1.17	2.8	0.005494

It is clear from the table that in all the three cases, ELM model outperforms the model with BP learning with respect to prediction accuracy and computation speed. Further, the ELM based models are found to be having compact network architecture with a smaller number of simulation parameters. Thus, ELM models are proved to be superior to BP based models in all aspects.

5 Conclusions

In this study, ANN models using extreme learning machine and back propagation algorithm have been developed to predict combustion pressure related parameters in dual spark ignition (DSI) engine which operates on varied percentage of ethanol blended with gasoline. The combustion pressure related parameters namely IMEP parameters (I_{MEP} and COV_{Imep}), maximum cylinder pressure parameters ($P_{ma,}$ COV_{pm} and Θ_{pm}) and maximum rate of pressure rise parameters ($[dP/d\Theta]_{m,}$ $COV_{[dP/d\Theta]m,}$ and $\Theta_{[dP/d\Theta]m}$) were obtained for 200 cycles at different loads, blends, compression ratios, spark timings at constant speed. Finally, the performance of models using two different learning algorithms is compared to arrive at the best ANN model.

Following conclusions are drawn from the current study:

- Models with ELM takes less time as compared to BP. Model-2 takes 0.004095 s compared to 0.596251s taken by Model-1, since ELM operates with single epoch.
- ELM based model provides the best possible performance with the least error. MAPE (%) on test data for Model-3 is 3.24 in contrast to 9.39 for Model-4.
- ELM based models have compact architecture taking a smaller number of hidden neurons. The optimum model architectures for Model-5 and Model-6 are 4:40:3 and 4:25:3 respectively.

References

[1] Sarwal R. Road Map for Ethanol Blending in India 2020-25: Report of the Expert Committee. NITI Aayog; 2021.

[2] Avanthi A, Venkata Mohan S. Emerging innovations for sustainable production of bioethanol and other mercantile products from circular economy perspective. Bioresource Technology. 2022, 363:128013.
[3] Sudip D. The national policy of biofuels of India-a perspective. Energy Policy. 2020, 143.
[4] Köten H, Karagöz Y, Balcı O. Effect of different levels of ethanol addition on performance, emission, and combustion characteristics of a gasoline engine. advances in mechanical engineering. 2020, 12.
[5] Bae C, Kim J. Alternative fuels for internal combustion engines. Proceedings of the Combustion Institute. 2017, 3(36):3389-3413.
[6] Iodice P, Amoresano A, Langella G. A review on the effects of ethanol/gasoline fuel blends on NO_X emissions in spark-ignition engines. biofuel research journal. 2021, 8(4):1465-1480.
[7] Iodice P, Senatore A, Langella G, Amoresano A. Advantages of ethanol-gasoline blends as fuel substitute for last generation Si engines. Environmental progress & sustainable energy. 2017, 36(4):1173-1179.
[8] Prasad S, Anoop S, Joshi HC. Ethanol as an alternative fuel from agricultural, industrial and urban residues. Resources, Conservation and Recycling. 2007, 50(1):1-39.
[9] Kumar CR, Nagarajan G. Performance and emission characteristics of a low heat rejection spark ignited engine fuelled with E20. Journal of Mechanical Science and Technology. 2012, 26(4):1241-1250.
[10] Sadiq MA, Ali YK, Noor AR. Effects of ethanol-gasoline blends on exhaust and noise emissions from 4-Stroke SI Engine. Engineering and Technology Journal. 2011, 29(7).
[11] Li H, Karim GA, Sohrabi A. The lean mixture operational limits of a spark ignition engine when operated on fuel Mixtures. Journal of engineering for gas turbines and power. 2009, 131(1).
[12] Ceviz MA, Yuksel F. Cyclic variations on LPG and gasoline-fuelled lean burn SI engine. Renewable Energy. 2006, 31(12):1950-1960.
[13] Zhuang Y, Qian YJ, Hong G. Lean burn performance of a spark ignition engine with an ethanol-gasolinedDual injection system. Energy & Fuels. 2018, 32(3):2855-2868.
[14] Heywood JB. Internal combustion engine fundamentals. McGraw-Hill Education; 2018.
[15] Schiffmann P. Root Causes of Cycle-to-Cycle combustion variations in spark ignited engines (Doctoral dissertation), 2016
[16] Ozdor N, Dulger M, Sher E. Cyclic variability in spark ignition engines: A literature survey. SAE transactions. 1994,103(3):1514-1552.
[17] Galloni E. Analyses about parameters that affect cyclic variation in a spark ignition engine. Applied Thermal Engineering. 2009, 29:1131-1137.
[18] Soltau JP. Cylinder pressure variations in petrol engines. Proceedings of the Institution of Mechanical Engineers: Automobile Division. 1960,14(1):99-117.
[19] Chen L, Pan J, Liu C, Shu G, Wei H. Effect of rapid combustion on engine performance and knocking characteristics under different spark strategy conditions. Energy. 2020, 192:116706.
[20] Yufeng G, Zongde F. Experimental study on different ignition system matching different spark plug gap. Proceedings of the 2009 International Conference on Computational Intelligence and Natural Computing 2009, 01:305-308.
[21] Duan X, Zhang S, Liu Y, Li Y, Liu J, Lai MC, Deng B. Numerical investigation the effects of the twin-spark plugs coupled with EGR on the combustion process and emissions characteristics in a lean burn natural gas SI engine. Energy. 2020, 206:118181.
[22] Crane D. Dictionary of Aeronautical Terms. Aviation Supplies & Academics. Inc., Newcastle. 2012.
[23] Harrington JA, Shishu RC, Asik JR. A study of ignition system effects on power, emissions, lean misfire limit, and EGR tolerance of a single-cylinder engine—multiple spark versus conventional single spark ignition. SAE Transactions. 1974, 837-845.
[24] Maji S, Sharma PB, Babu MK. A Comparative study of performance and emission characteristics of CNG and gasoline on a single cylinder SI Engine. SAE Technical Paper; 2004.
[25] Raja AS, Arasu AV, Sornakumar T. Effect of gasoline-ethanol blends on performance and emission characteristics of a single cylinder air cooled motor bike SI engine. Journal of Engineering Science and Technology. 2015, 10(12):1540-1552.
[26] Shang H, Zhang L, Chen X, Guo P, Zhang H. Experimental investigation about effect of double-spark plug ignition on cyclic variation and knocking for SI engine. Sādhanā. 2021, 46:1-3.

[27] Altın İ, Bilgin A, Sezer İ. Theoretical investigation on combustion characteristics of ethanol-fueled dual-plug SI engine. Fuel. 2019, 257:116068.
[28] Aisyah IS, Setiyoadi W, Suwarsono S. Performance of four stroke one-cylinder ic engine with dual spark plugs using 94–100% Ethanol. J. Energy Technology. Policy. 2016, 6:13-17.
[29] Kannan GR, Balasubramanian KR, Anand R. Artificial neural network approach to study the effect of injection pressure and timing on diesel engine performance fuelled with biodiesel. International Journal of Automotive Technology. 2013, 4(14):507-519.
[30] Pacheco-Vega A, Sen M, Yang KT, McClain RL. Neural network analysis of fin-tube refrigerating heat exchanger with limited experimental data. International Journal of Heat and Mass Transfer. 2001, 44(763):770.
[31] Agatonovic-Kustrin S, Beresford R. Basic concepts of artificial neural network (ANN) modelling and its application in pharmaceutical research. Journal of Pharmaceutical and Biomedical Analysis. 2000, 22(5):717-727.
[32] Anderson JA. An Introduction to Neural Networks. MIT Press. Cambridge, MA., ISBN. 1995, 10:0262011441.
[33] HAYKIN S. A Comprehensive Foundation. Neural Networks. 1994.
[34] Can O, Baklacioglu T, Ozturk E, Turan O. Artificial neural networks modelling of combustion parameters for a diesel engine fueled with biodiesel fuel. Energy. 2022, 247:123473.
[35] Liu J, Huang Q, Ulishney C, Dumitrescu CE. Machine learning assisted prediction of exhaust gas temperature of a heavy-duty natural gas spark ignition engine. Applied Energy. 2021, 300:117413.
[36] Kalogirou SA. Artificial intelligence for the modelling and control of combustion processes: a review. Progress in energy and combustion science. 2003, 29(6):515-566.
[37] Huang GB, Zhu QY, Siew CK. Extreme learning machine: Theory and applications. Neurocomputing. 2006, 70:489-501.
[38] Deng C, Huang G, Xu J, Tang J. Extreme learning machines: new trends and applications. Science China information sciences. 2015, 2(58):1-16.
[39] Deng WY, Ong YS, Zheng QH. A Fast-Reduced Kernel Extreme Learning Machine. Neural Networks. 2016, 100(76):29-38.
[40] Sebayang AH, Masjuki HH, Ong HC, Dharma S, Silitonga AS, Kusumo F, Milano J. Prediction of engine performance and emissions with Manihot glaziovii bioethanol-Gasoline blended using extreme learning machine. Fuel. 2017, 210:914-921.
[41] Zeng W. Efficient and Accurate Neural Network Based Internal Combustion Engine Modelling and Prediction,2021
[42] Mariani VC, Och SH, Coelho LD, Domingues E. Pressure prediction of a spark ignition single cylinder engine using optimized extreme learning machine models. Applied Energy. 2019, 249:204-221.
[43] Silitonga AS, Masjuki HH, Ong HC, Sebayang AH, Dharma S, Kusumo F, Siswantoro J, Milano J, Daud K, Mahlia TM, Chen WH. Evaluation of the engine performance and exhaust emissions of biodiesel-bioethanol-diesel blends using kernel-based extreme learning machine. Energy. 2018, 159:1075-1087.
[44] Zhao K, Shen T. Application of extreme learning machine to knock probability control of SI combustion engines. In Proceedings of ELM 2019, Springer International Publishing 2021, 109-122.
[45] Janakiraman VM, Nguyen X, Assanis D. An ELM based predictive control method for HCCI engines. Engineering Applications of Artificial Intelligence. 2016, 48:106-118.
[46] Aghbashlo M, Shamshirband S, Tabatabaei M, Yee L, Larimi YN. The use of ELM-WT (extreme learning machine with wavelet transform algorithm) to predict exergetic performance of a DI diesel engine running on diesel/biodiesel blends containing polymer waste. Energy. 2016, 100(94):443-456.
[47] Zheng J, Huang Z, Wang J, Wang B, Ning D, Zhang Y. Effect of compression ratio on cycle-by-cycle variations in a natural gas direct injection engine. Energy & fuels. 2009, 23(6):5357-5366.
[48] Duan XB, Liu JP, Yuan ZP, Guo GM, Liu Q, Tang QJ, Deng BL, Guan JH. Experimental investigation of the effects of injection strategies on cycle-to-cycle variations of a DISI engine fuelled with ethanol and gasoline blend. Energy. 2018, 165:455-470.

[49] Chang WC. An improved method of investigation of combustion parameters in a natural gas fuelled SI engine with EGR and H2 as additives (Doctoral dissertation, University of Birmingham), 2002
[50] Han SB. Cycle-to-cycle variations under cylinder-pressure-based combustion analysis in spark ignition engines. Journal of Mechanical Science and Technology. 2000, 10(14):1151-1158.
[51] AL-Baghdadi MS. Measurement and prediction study of the effect of ethanol blending on the performance and pollutants emission of a four-stroke spark ignition engine. Proceedings of the Institution of Mechanical Engineers. Part D, Journal of automobile engineering. 2008, 222(5):859-873.
[52] Petkovic D, Madic M, Radovanovic M, Gecevska V. Application of the performance selection index method for solving machining MCDM problems. Facta Universitatis, Series: Mechanical Engineering. 2017, 15(1):97-106.
[53] Huang GB, Zhu QY, Siew CK. Extreme learning machine: a new learning scheme of feedforward neural networks. In 2004 IEEE international joint conference on neural networks (IEEE Cat. No. 04CH37541) 2004, 2:985-990.
[54] Kennedy J, Eberhart R. Particle swarm optimization. In Proceedings of ICNN'95-international conference on neural networks IEEE 1995, 4:1942-1948
[55] Cambria E, Huang GB, Kasun LL, Zhou H, Vong CM, Lin J, Yin J, Cai Z, Liu Q, Li K, Leung VC. Extreme Learning Machines. IEEE Intelligent Systems. 2013, 6(28):30-59.
[56] Javed K, Gouriveau R, Zerhouni N. SW-ELM: A summation wavelet extreme learning machine algorithm with a priori parameter initialization. Neurocomputing. 2014, 123:299-307.
[57] Wan C, Xu Z, Pinson P, Dong ZY, Wong KP. Probabilistic forecasting of wind power generation using extreme learning machine. IEEE Transactions on Power Systems. 2013, 29(3):1033-1044.
[58] Huang G, Huang GB, Song S, You K. Trends in extreme learning machines: A review. Neural Networks. 2015, 61:32-48.